ELSEVIER

Deep-Sea Research II 52 (2005) 757–780

DEEP-SEA RESEARCH
PART II

www.elsevier.com/locate/dsr2

Linking oceanic food webs to coastal production and growth rates of Pacific salmon (*Oncorhynchus* spp.), using models on three scales

Kerim Y. Aydin[a,*], Gordon A. McFarlane[b], Jacquelynne R. King[b], Bernard A. Megrey[a], Katherine W. Myers[c]

[a]*Alaska Fisheries Science Center, US National Marine Fisheries Service, Seattle, WA, USA*
[b]*Pacific Biological Station, Fisheries and Oceans Canada, Nanaimo, British Columbia, Canada*
[c]*High Seas Salmon Project, School of Aquatic and Fisheries Sciences, University of Washington, Seattle, WA, USA*

Accepted 17 December 2004
Available online 8 March 2005

Abstract

Three independent modeling methods—a nutrient-phytoplankton–zooplankton (NPZ) model (NEMURO), a food web model (Ecopath/Ecosim), and a bioenergetics model for pink salmon (*Oncorhynchus gorbuscha*)—were linked to examine the relationship between seasonal zooplankton dynamics and annual food web productive potential for Pacific salmon feeding and growing in the Alaskan subarctic gyre ecosystem. The linked approach shows the importance of seasonal and ontogenetic prey switching for zooplanktivorous pink salmon, and illustrates the critical role played by lipid-rich forage species, especially the gonatid squid *Berryteuthis anonychus*, in connecting zooplankton to upper trophic level production in the subarctic North Pacific. The results highlight the need to uncover natural mechanisms responsible for accelerated late winter and early spring growth of salmon, especially with respect to climate change and zooplankton bloom timing. Our results indicate that the best match between modeled and observed high-seas pink salmon growth requires the inclusion of two factors into bioenergetics models: (1) decreasing energetic foraging costs for salmon as zooplankton are concentrated by the spring shallowing of pelagic mixed-layer depth and (2) the ontogenetic switch of salmon diets from zooplankton to squid. Finally, we varied the timing and input levels of coastal salmon production to examine effects of density-dependent coastal processes on ocean feeding; coastal processes that place relatively minor limitations on salmon growth may delay the seasonal timing of ontogenetic diet shifts and thus have a magnified effect on overall salmon growth rates.

*Corresponding author.
E-mail address: kerim.aydin@noaa.gov (K.Y. Aydin).

0967-0645/$ - see front matter © 2005 Elsevier Ltd. All rights reserved.
doi:10.1016/j.dsr2.2004.12.017

1. Introduction

The biological production and carrying capacity of the pelagic food webs of the subarctic Pacific gyres have been subjects of considerable speculation, especially given the relatively limited data collection performed in these high-seas areas (Pearcy et al., 1999). This interest has been driven in part by the fact that the gyres are a rearing and growth area for Pacific salmon (*Oncorhynchus* spp.) and are therefore production areas for important commercial fisheries. Additionally, the link between climate and fisheries on decadal scales points to important ecosystem interactions occurring within the gyres and in synchrony with Pacific-wide events (e.g., the Pacific Decadal Oscillation, Mantua et al., 1997).

Attempts to quantify the maximum production rates of fish in the gyres have revealed a fundamental paradox. Calculations of zooplankton biomass and production, when compared to demands made by foraging salmon, invariably indicated a surplus of available food. A model constructed in the 1970s (Favorite and Laevastu, 1979) concluded that the North Pacific could sustain 10 times the 1970s standing stock of salmon. Yet during the 1980s and 1990s, when the system contained twice the total salmon biomass examined by Favorite and Laevastu (1979), body sizes declined (Bigler et al., 1996; Ishida et al., 1993; Ricker, 1995).

Conservative production estimates, using observed 1980s and 1990s zooplankton and salmon biomass, indicate that adult salmon consume between 0.04% and 0.10% of available annual zooplankton production (Brodeur et al., 1999). Since salmon are a dominant pelagic nekton in the region, it seemed unlikely that this level of consumption would lead to competition for prey and thus represent an ecosystem at its carrying capacity for salmon.

However, links between species may not be linear or direct, and may cross multiple scales. Specifically, Pacific salmon spend their early life history at sea in coastal waters before migrating to the open ocean to feed. While these fish may put on 90% or more of their body weight in oceanic areas, their mortality may be highest and thus their numerical carrying capacity determined through coastal processes or through critical bottlenecks such as their first winter at sea (Beamish and Mahnken, 2001). Further, the rapid growth of salmon at sea provides the fish with opportunities for ontogenetic shifts in foraging behavior that may lead to complex food web dynamics.

Moreover, it is clear that environmental forcing on multi-year time scales affects the biology of higher trophic levels in these ecosystems and across the globe (Beamish, 1993; Brodeur and Ware, 1995; Hollowed et al., 1998; Francis et al., 1998; Beamish et al., 1999). The effects of climate are not limited to the direct increase or decrease of the biomass of the entire system. Animals with multi-year life histories integrate short-term changes, and their biomass may not respond immediately to changes in ocean conditions. In order to move from correlative to mechanistic relationships linking climate and biology, it is necessary to construct models, either conceptual or quantitative, which link appropriate scales of time and space into interactions modeled through food webs.

The subarctic north Pacific consists of a major cyclonic gyre surrounded on the north by coastline and boundary currents and on the south by the Subarctic Current, which isolates the gyres from subtropical waters. The main gyre is pinched at its longitudinal center by the Aleutian Islands, which causes recirculation of its waters into two subgyres: the Western Subarctic and Eastern (Alaskan) Subarctic Gyres (Fig. 1).

In the eastern subarctic, Ocean Station P (50°N, 145°W) was the subject of long-term plankton monitoring in the 1960s and 1970s and has been a sampling location for salmon research surveys throughout the 1980s and 1990s, and was thus chosen as the focal point for modeling. The time period targeted for data inclusion in the models was the 1990s, although in many cases the lack of 1990s data led to the use of information from earlier time periods. During this time period, Pacific salmon overall biomass was high, water temperatures were warm, and overall summer zooplankton standing stocks were relatively high (Brodeur and Ware, 1995; Francis et al., 1998).

The waters around Ocean Station P are more heavily influenced by the eastward-moving

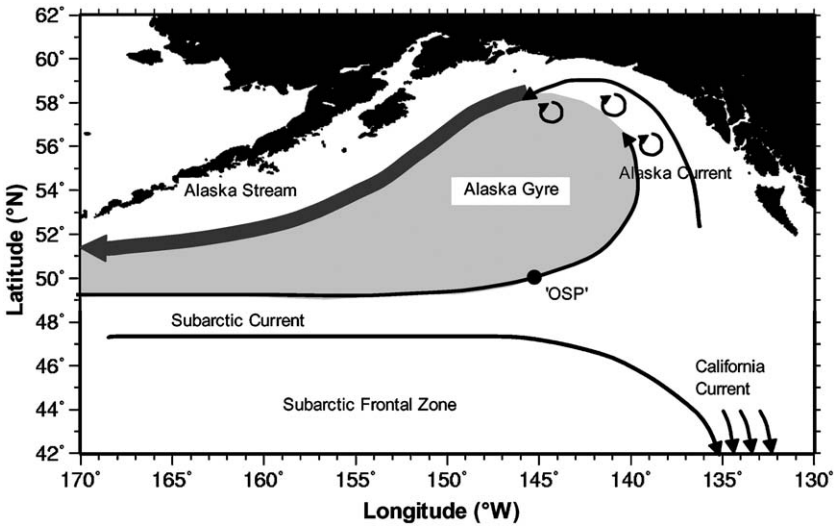

Fig. 1. The eastern subarctic Pacific (Alaskan) Gyre, showing approximate location of major currents and Ocean Station P (50°N, 145°W).

Subarctic Current than the more northerly waters of the central Alaskan gyre. This is a region in which foraging Pacific salmon stocks may mingle and compete with transitional and central North Pacific species; potential competitors such as neon flying squid (*Ommastrephes bartrami)* and important forage species, especially the gonatid squid *Berryteuthis anonychus* (Pearcy et al., 1988). Moreover, Station P is near the southern limit of summer salmon distribution for some species, which may be strongly controlled or correlated with water temperature (Welch et al., 1998). Therefore, it is worth examining how salmon growth might be affected by climatic shifts, either through direct effects of temperature on salmon growth or relative to changes in prey supply or biogeographic overlap (Aydin et al., 2000).

"Whole ecosystem" marine food web modeling has generally been based on the principle of stationary ecosystems; that is, models in which energy flow is tracked between species within an unmoving oceanic box, self-contained with the exception of raw energy input (sunlight and/or nutrients) and dissipation (respiration). Various conceptual food web models of the Alaskan gyre have been constructed (Sanger, 1972; Pauly and Christensen, 1996; Brodeur et al., 1999), usually with a combination of quantitative and qualitative data. In a sense this current paper is the latest in this tradition.

On the other hand, models of highly migratory species, such as Pacific salmon (*Oncorhynchus* spp.), by necessity follow moving animals or cohorts through the environments that they encounter during their life cycle. To examine indirect and possibly unexpected interactions between migratory species and ecosystem production, food web models may be a useful initial tool. However, to extend to appropriate scales, multiple models should be examined in concert, with models covering small- or short-scale dynamics (such as plankton blooms) being combined with models following the growth of individual cohorts of salmon and annual ecosystem-wide energy budgets.

In this paper, we link three modeling methods to examine oceanic processes in the eastern subarctic (Alaskan) Gyre in the 1990s. With the first method, Ecopath, we construct a quantitative pelagic food web and in doing so synthesize disparate data sources to create a "snapshot" of energy flows within the region. Then, output from a nutrient-Phytoplankton–Zooplankton (NPZ) model, NEMURO (Fujii et al., 2002; Yamanaka

et al., 2003), is used to drive a seasonal cycle that is connected to the food web using Ecopath's dynamic cousin Ecosim. Finally, we build a bioenergetics model of pink salmon (*Oncorhynchus gorbuscha*) into the Ecosim routines, so that ontogenetic and seasonal feedback occurs between the models of salmon growth and ecosystem production. Prey availability from Ecosim is used to determine pink salmon consumption and growth rates for the bioenergetics model, which in turn determines ontogenetic diet preferences and thus affects seasonal prey depletion rates in the running Ecosim simulations (Fig. 2).

The eventual goal of building linked, mechanistic models is to isolate and test climatic factors that contribute to variation in ocean fish production, for example, to determine how coastal variation in salmon survival might affect the carrying capacity for salmon in the Pacific basin.

Here, as a first step, we present a system of models that use varying levels of coastal pink salmon production (numbers and size), interacting with the timing of seasonal production and prey availability, predation, and competition, as input drivers for ocean salmon growth. Using this approach, we explore hypothesis for the controlling factors underlying fish production, to help examine the overall effects of long-term climate variation on wide-ranging species in the subarctic Pacific basin.

2. Methods

2.1. Ecopath modeling

The construction of the Ecopath model of the eastern Subarctic gyre (ESAG) was an iterative process of data gathering and examination conducted in a series of workshops held by the North Pacific Marine Science Organization (PICES) Basin Ecosystems (BASS) Task Team. A similar model for the western Subarctic gyre (WSAG) was built in parallel, although results from the WSA are not presented here. The data synthesis for the models was thus the result of an international collaboration with a wide range of scientists

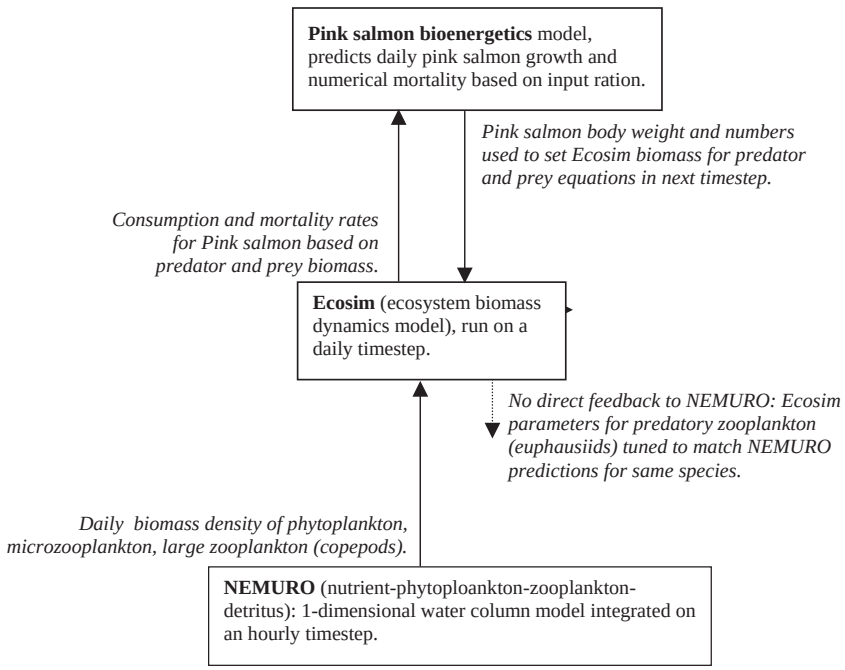

Fig. 2. Linking schematic for the three modeling techniques used in this study.

familiar with the subarctic ecosystems. The full modeling process for both the ESAG and WSAG, including data sources, parameter estimation methods, and results, is described in Aydin et al. (2003).

Ecopath is a food-web modeling tool that has gained recognition as a method for synthesizing marine food-web data (Polovina, 1985; Christensen and Pauly, 1992; Christensen et al., 2000). Ecopath assists in the construction of a quantitative food web by requiring that the biomass inputs and outputs of each ecosystem component (functional group or species), when adjusted for measured biomass accumulation or loss, provide a consistent accounting within the specified range of uncertainty in the data (the mass-balance criterion). The model's strength lies in its ability to combine and compare data common to many types of fisheries analyses, especially stock assessment and food habits studies, into a single coherent picture or ecosystem "snapshot."

Ecopath's mass-balance criterion is applied by solving a simple set of linear equations that quantify the amount of material (measured in biomass, energy or tracer elements) moving in and out of each compartment (functional group) in a modeled food web. A single functional group (food web compartment) may be a single species or a set of trophically similar species. The master Ecopath equation is, for each functional group (i) with predators (j):

$$B_i\left(\frac{P}{B}\right)_i \cdot \mathrm{EE}_i + \mathrm{IM}_i + \mathrm{BA}_i = \sum_j \left[B_j \cdot \left(\frac{Q}{B}\right)_j \cdot \mathrm{DC}_{ij}\right] + \mathrm{EM}_i + C_i.$$

Here, B is the biomass of a species, P/B the production/biomass ratio (commonly set equal to mortality Z), IM and EM are immigration and emigration, Q/B is the consumption/biomass ratio, DC diet composition, C is fisheries catch, and BA is biomass accumulation, which may be positive or negative. The units of biomass may be energy, matter, or nutrient based; in this model the units are wet weight per unit area (t/km^2) and the timescale for production rates is yearly.

EE, ecotrophic efficiency, is a measure of the difference between a functional group's production and modeled loss to other ecosystem components or fisheries. An EE of 1.0 indicates that all of a group's yearly assimilated production has an accounted source of mortality or accumulation. An EE <1.0 indicates that a functional group's annual accounted gains are greater than its losses. As senescence is not explicitly considered, it is ecologically reasonable for EE to be less than 1.0 even in the absence of biomass accumulation: for top predators in the absence of fishing, EE will be 0 by definition. The use of EE as a model diagnostic is described in Appendix A.

The mass-balance constraints of Ecopath do not in themselves require or assume that the modeled ecosystem is in equilibrium, but rather require that any directional component (known increase or decrease of biomass) is included in the mass-balance accounting through the biomass accumulation (BA) term. However, in practice, especially in systems with sparse data such as the subarctic gyres, the necessary averaging of data over longer (climatic regime-scale) time periods requires an added assumption of relative stability.

Within a modeled regime, it is assumed that a modeled ecosystem lies close (within the range of short-term process noise) to an attractive and relatively stable equilibrium for all modeled biomass components. The system is not assumed to exist in this state in any given instant; rather, like a carrying capacity for an individual species, it is the state towards which the ecosystem would tend in the absence of driving perturbations (e.g., changes in fishing rates, climate, or other process-related noise). The food webs created are similar to those created through other synthetic methods: the resulting models represent a snapshot of what is essentially a moving target, a changing ecosystem.

For the ESAG model, no attempt was made to adjust or balance the input parameters based on mass-balance concerns during this initial data gathering and preparation. The results of this initial phase was an unbalanced model; that is, a quantitative food web for which many of the functional groups' EEs were far greater than 1.0, indicating potential errors in the input data or incorrect/incomplete model formulation. These unbalanced models were presented at an initial

workshop and, based on discussion of data quality and sources, adjustments were made to balance the model (reduce all EEs below 1.0).

After conducting this initial balancing exercise, metrics of ecosystem structure, such as community respiration, production, trophic level, and niche habitat, were calculated from the balanced models of the two ecosystems. Further, initial Ecosim runs (perturbation analyses) were performed. The results of these runs with the initial balanced models often highlighted connections in the model, which were felt by workshop participants to be inaccurate, represent model pathologies, or not accord with limited historical data and/or experience. After this workshop, additional data sources were targeted and provided, which helped to clarify many of these data gaps. Thus, several generations of balanced models were produced and subjected to the similar tests before the final workshop produced "completed" ESAG model.

2.2. Ecosim

This assumption of relative stability becomes a formal constraint in the extension of the Ecopath model to dynamic predictions through the use of Ecosim. Ecosim uses the mass-balance solution to the Ecopath master equations to derive the parameters that are used in the following biomass dynamics model:

$$\frac{dB_i}{dt} = GE_i \sum_{j \in prey} \left[f_{ij}(\overline{B}) \right] - \sum_{k \in pred} \left[f_{ki}(\overline{B}) \right] + PP(B_i) + IM(B_i) - EM(B_i) - F_{i,t,}B_i - M_{0i}B_i.$$

The definitions of these parameters and functions may be found in Table 1. This general model does not automatically assume that an equilibrium state exists for all functional groups in the ecosystem. In particular, the predator/prey interaction functions $f(B)$ are set from consumption, production, and diet parameters plus an additional

Table 1
Parameters and functional forms used in the Ecosim model, as described in Walters et al. (1997)

Parameter	Abbreviation	Notes
Growth efficiency	GE	Constant for each predator, calculated as $(P/B)/(Q/B)$ from Ecopath balance; may be subject to time forcing.
Consumption equation	$f(B) = (Q_{pred} \cdot DC_{pred,prey,base} \cdot (B_{pred}/B_{predbase}) \cdot (B_{prey}/B_{preybase}) \cdot X_{pred,prey}/((X_{pred,prey} - 1) + (B_{pred}/B_{predbase}))$	As documented in Walters et al. (1997), independent terms for each predator/prey link include predator density dependence. Calibrated from Ecopath Q/B and diet composition. $X_{pred,\ prey}$ determines the degree toward which feeding is ratio dependent (X close to 1) or Lotka-Volterra ($X \gg 2$). Handling time (dependent on sum of prey) and other adjustments or forcing are possible as documented in the EwE manual.
Primary production rate	PP	Simple density-dependent half-saturation curve for all primary producers.
Immigration	IM	Constant yearly rate independent of biomass (assumed determined by outside dynamics). Determined from input Ecopath immigration.
Emigration	EM	Per-biomass rate determined from input Ecopath emigration.
Biomass accumulation	BA	Per-biomass rate determined from input Ecopath biomass accumulation.
Fishing mortality	F	Per-biomass rate determined from input Ecopath fisheries catch and biomass.
"Other" (not predation) natural mortality	M_o	Determined by Ecopath ecotrophic efficiency and used to ensure equilibrium in the absence of biomass accumulation.

term, vulnerability, which represents the relative strength of top-down (Lotka–Volterra) interactions and bottom-up (density-dependent ratio) interactions (examples of using these functions to vary top-down and bottom-up control may be found in Shannon et al., 2000; Cox et al., 2002). Further, the relative importance of foraging time limitation or handling time may be introduced into $f(B)$ as tunable parameters (Walters et al., 1997).

In theory, the use of these functions does not guarantee that the system has an equilibrium state, and the above formulae may include oscillatory or chaotic dynamics. However, in practice, the transition between Ecopath and Ecosim parameters defaults so as to ensure the ecosystem is near equilibrium.

Specifically, the foraging interactions at the heart of the dynamic model $f(B)$ assume that each functional group (species) maintains constant "internal" dynamics such as age structure and forage preference. For exploring small perturbations from steady-state conditions, or interannual shifts in predation mortality arising from changes in sustained fishing pressure, such assumptions may be reasonable. However, for the modeling of seasonal dynamics or the explicit growth of species that spend a limited portion of their life cycle within the modeled gyre boundaries extensions to the model are necessary.

To this end, we implemented the Ecosim equations independently from the Ecopath with Ecosim package developed by Christensen et al. (2000). Specifically, for capturing seasonal dynamics we implemented an Adams-Basforth numerical integration routine (Atkinson, 1989) on a daily timestep, rather than using the default monthly Ecosim timestep. Moreover, we explored alternative functional responses to the Arena formulation described by Walters et al. (1997), in order to allow interface with NEMURO and bioenergetics models.

2.3. NEMURO

Modeling the seasonal dynamics of plankton blooms through NPZ models has a developed history. Specifically for this experiment, the NEMURO model (Fujii et al., 2002; Yamanaka et al., 2003) was reparameterized to capture the detailed seasonal dynamics of Ocean Station P. The NEMURO outputs used here are described in Appendix E of Aydin et al., (2003) (Appendix A) and compare favorably to 1990s production estimates described by Wong et al. (1995). NEMURO includes nutrient recycling and mixed-layer depth dynamics integrated on an hourly timestep, as such it provides a more thorough exploration of seasonal plankton production than Ecosim for the Alaskan Gyre.

The NEMURO seasonal model was used in the Ecopath building stage, as described in Aydin et al. (2003), to provide annual production and standing stock inputs for the following Ecopath functional groups: small (micro-) phytoplankton; large phytoplankton; small (micro-) zooplankton; large zooplankton (copepods); and predatory zooplankton (euphausiids, amphipods, and pteropods). As NEMURO was used to provide the annual averages for the initial Ecopath model, reintroducing seasonal cycles from NEMURO into Ecosim should be consistent with the annual averages used in the Ecopath balance.

Rather than linking NEMURO and Ecosim models directly, we added seasonality to the Ecosim model by forcing (setting) daily biomass levels for Ecosim phytoplankton, microzooplankton, and copepods to NEMURO outputs for each daily timestep. Predatory zooplankton (euphausiids, amphipods, and pteropods) were modeled independently in NEMURO and Ecosim, and the results compared to ensure that Ecosim output, when forced by NEMURO, was comparable to NEMURO itself for this functional group.

Thus, NEMURO provided a one-way input for driving the daily timesteps of Ecosim. The only inconsistency in this method is that the NEMURO and Ecosim detrital cycles (nutrient recycling) were incompatible. However, for this pelagic ecosystem, the nutrient recycling occurs in the NEMURO-forced trophic levels only, so any functional groups in Ecosim that depended on detrital supply were overridden by NEMURO inputs.

2.4. Linking bioenergetics and Ecosim

Bioenergetics models combine laboratory-measured physiological parameters with field-measured environmental data to determine an

instantaneous daily rate of somatic growth for a given species, fed a given ration in a given environment. Parameter sets for many fish have been published (cf. Hewett and Johnson, 1992). For the first implementation of an Ecosim/bioenergetics linkage, we chose to model growth for North American stocks of pink salmon.

Pink salmon were chosen due to their relatively simply life cycle in the Alaskan Gyre. Pink salmon from North American stocks generally enter the Alaskan Gyre from coastal waters in late summer, and spend one winter in the gyre before putting on 80%+ of their body weight during the following the spring and summer before migrating to spawn (Ishida et al., 1998). Thus, maturation age and multi-year life histories did not have to be considered. For the simulation described here, salmon other than pink salmon continued to be modeled with the original Ecosim formulation; future modeling may extend this technique to salmon species with more complex life histories.

Bioenergetics models calculate a daily energy balance by assuming that all energy entering and leaving a fish must be accounted for. The general model formula is

$$C = G + R + F + U,$$

where C is a fish's daily consumption (in food calories), G is the expected growth, and R (respiration) and $F + U$ (egestion and excretion) are heat and material losses respectively, arising from the process of metabolism. The benefit of bioenergetics modeling is that R and $F + U$ can been parameterized from laboratory experiments as exponential functions of C, G, water temperature, and fish body size. The formulae, parameters and references for the models used for pink salmon are given in Beauchamp et al. (1989). Given the following four input variables for a salmon:

- ambient water temperature,
- daily ration (C in the equation above),
- prey quality (caloric density and the proportion that is indigestible),
- body weight of the salmon,

the bioenergetics model will predict the amount of somatic growth (G) experienced by the fish, and estimate the conversion efficiency of growth (material assimilated/material consumed). The bioenergetics model we implemented was parameterized for a daily time increment; the linking itself was performed in Microsoft Visual Basic® along with our implementation of the Ecosim algorithms.

As with NEMURO in the lower trophic levels, bioenergetics models were initially used in Aydin et al. (2003) to calculate annual average P/B and Q/B values in the initial Ecopath formulation of Pacific salmon. Therefore, if diet remains constant over a season, the explicit bioenergetics implementation simply divides yearly Ecosim P/B and Q/B values back into daily rates, and these rates should remain consistent with the annual averages in the initial Ecopath formulation. However, the explicit dynamic linkage of Ecosim to seasonal diets would be expected to have profound effects on overall salmon growth rates, especially with respect to predicted changes in seasonal bottlenecks that might vary with climate.

Coastal input of each yearly pink salmon cohort into the Alaskan Gyre was assumed to occur on August 15 of each year (Heard, 1991), with the entrance of single cohort consisting of identical fish with an initial body weight of 37.5 g (Table 2; Fig. 3). Only a single value for body weight was tracked for the cohort throughout the simulations; later models may include statistical distributions for growth.

The number of fish entering the gyre was hindcast so that, assuming an annual adult mortality rate of 2.45 (Bradford, 1995) and monthly body weights in Table 2, the number of entering fish was set to ensure that the biomass of pink salmon, averaged over all months, was equal the biomass density of the balanced Ecopath model. This maintained internal consistency, as the Ecopath model's initial biomass was calculated using the same hindcast method on reported 1990s catch + escapement levels of North American pink salmon (Rogers, 2001).

For the purpose of this study, diet data for pink salmon were only used from fish collected in an area around Ocean Station P that was south of 53°N and between 140 and 160°W, inclusive. As found by Pearcy et al. (1988) and Aydin et al.

Table 2
Mean subarctic Pacific body weights (mean and standard deviation) of pink salmon by month, from high seas research gillnets (Ishida et al., 1998)

Month	Body weight (g)	s.d.	*N*		
			(millions)	N/km^2	t/km^2
Jul	31.8	5.8	1159	320	0.010
Aug	39.5	27.5	945	261	0.010
Sep	58.1	25.5	770	213	0.012
Oct	138.7	40.7	628	173	0.024
Nov	145.7	38.5	512	141	0.021
Dec	172.9	81.4	418	115	0.020
Jan	154.9	36.7	340	94	0.015
Feb	318.5	93	278	77	0.024
Mar	408.3	153.7	226	62	0.026
Apr	584.5	184.8	185	51	0.030
May	777.6	232.3	150	42	0.032
Jun	919.0	252.3	123	34	0.031
Jul	1128.9	322.5			
Aug	1320.6	336.6			
Sep	1523.1	397.6			

Numbers of pink salmon at sea are hindcast based on a catch + escapement of 100 million North American fish (approximate 1990s returns) and a yearly instantaneous mortality rate of 2.45. Biomass density (tons/km^2) is based on a total eastern Subarctic Pacific area of 3,622,000 km^2.

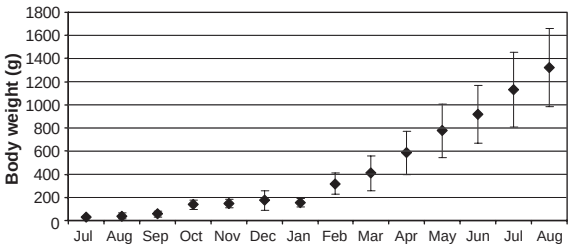

Fig. 3. Mean subarctic Pacific body weights (mean and standard deviation) of pink salmon by month, from high seas research gillnets (Ishida et al., 1998).

(2000), 53°N is the approximate latitude of a moving oceanographic boundary, which has importance for salmon feeding. South of this latitude, near Ocean Station P, maturing salmon, especially pink, sockeye (*O. nerka*), and coho (*O. Kisutch*) salmon, feed heavily on micronektonic squid, primarily the gonatid squid *B. anonychus*. North of this boundary, in the center of the Alaskan gyre, pink and sockeye salmon feed primarily on zooplankton, while coho eat little until they reach the continental shelf. Previous bioenergetics modeling has shown that feeding on this lipid rich squid species may be critical for salmon to maintain high growth rates (Aydin, 2000).

The largest collection of diet data came from the July surveys of the Japanese research vessel *Oshoro maru*, 1980–2001 (Pearcy et al., 1988; Aydin et al., 2000; Kaeriyama et al., 2004). Extensive research conducted between 1950 and 1970 indicated that large seasonal changes occur in salmon diets (LeBrasseur, 1966, 1972). Unfortunately, almost no diet data existed for fall and spring for the 1980–2001 time period.

Initially, we decided against using the 1950–1970 data set in these models, as a general additive model (GAM) analysis between the 1950–1970 and 1980–2001 datasets indicated significant dietary differences in salmon between different climatic "regimes" (Aydin, 2000). Additional diet data were incorporated from three research cruises conducted in the 1990s: the *Kaiyo maru* cruises of December 1992 and January 1996 and the *Great Pacific* cruise of May 1998 (Myers, 1993; Myers, 1996; Ocean Carrying Capacity Program, 1998). The December 1992, diet data was taken as a proxy for September–December diet preferences, and February–April diets were modeled by a weighted average of January and May data. As described in the results, we later incorporated April data from the 1950–70 data set.

On each simulation day after August 15, the following steps were performed (see Fig. 2):

1. Ecosim reference diet compositions (preferences) for the pink salmon cohort were updated based on the body weight of the cohort and ontogenetic diet preferences (see Section 3 for the functional forms used to simulate prey switching based on diet data).
2. Ecosim functional responses (Table 1) were used to calculate the total consumption of prey by the pink salmon cohort and the mortality of pink salmon by predators, based on the total biomass of pink salmon, the biomass of each prey and predator type (forced by NEMURO

Table 3
Caloric compositions of prey items used for bioenergetics model, and range of caloric compositions of prey found in salmon stomachs in subarctic Pacific waters (Davis, 2003)

Prey group	Cal/g wet weight	Species and range
Copepods	700	*Neocalanus cristatus*, 627–748
Euphausiids	1000	*Thysanoessa* spp., *Euphausia* spp., 840–1050
Pteropods	650	*Limacina helicina*; 624–940
Amphipods	800	*Parathemisto pacifica*; 852–1010
Ctenophores	50	*Beroe* sp., 47
Salps	36	*Salpa* sp., 36
Chaetognaths	450	*Sagitta elegans*; 455–488
Pelagic forage fish	1200	*Gasterosteus aculeatus*; 1166–1533
Mesopelagic forage fish	2000	*Stenobrachius leucopsarus; Tarletonbeania crenularis; Leuroglossus schmidti*; 2041–2365 (Bering Sea)
Micron. squid	1500	*Berryteuthis anonychus*; 1307–1737 (increases with increasing mantle length).

or resulting from Ecosim), and the Ecosim reference diet compositions set in step 1. However, for the initial runs the density-dependent term for pink salmon foraging ($X_{i,\ \mathrm{pink}}$ in $F(B)$ equation of Table 1) was set so pink salmon foraging showed pure Lotka–Volterra interactions and no density-dependence ($X_{i,\ \mathrm{pink}} \gg 25.0$). Handling time (as implemented by the Holling Type II functional response) was not used, as metabolic costs were calculated by the bioenergetics model in step 3, (below) and reduced effective feeding gains for salmon feeding at rations higher than satiation.

3. The total prey consumption calculated for pink salmon in step 2, the current cohort body weight, cohort numbers, prey caloric density, and water temperature, were input into the bioenergetics routines to calculate the new body weight of the cohort. Prey caloric density was calculated from diets determined in step 2 and measured prey caloric densities in the ESAG (Table 3). Water temperature was modeled as a sine curve fit to weekly $1 \times 1^{\circ}$ sea-surface temperature (SST) at 50°N, 145°W, 1982–1998 (Fig. 4; IGOSS, 2000). Future model runs may examine the effects of using deeper-water temperatures to account for the daily vertical migrations of salmon.
4. Mortality was applied to pink salmon cohort numbers based on predation and 'other' mortality calculated in Step 2. Initially, the other mortality term (M_0) for pink salmon was adjusted downwards from the Ecosim default so that average annual mortality was equal to 2.45; this adjustment was necessary to account for the difference between mortality in terms of numbers and mortality in terms of biomass input into the initial Ecopath model.
5. All other species biomasses were updated from the standard Ecosim numerical integration routines (Adams–Basforth with a daily time-step), or in the case of lower trophic levels, from the daily NEMURO output biomass levels. For the Ecosim functional response, the "default" parameters for the Walters et al. (1997) arena functional response were used (all functional responses at half-saturation between ratio-dependent and Lotka–Volterra formulations; $X_{ij} = 2$ for all predator/prey pairs). In these

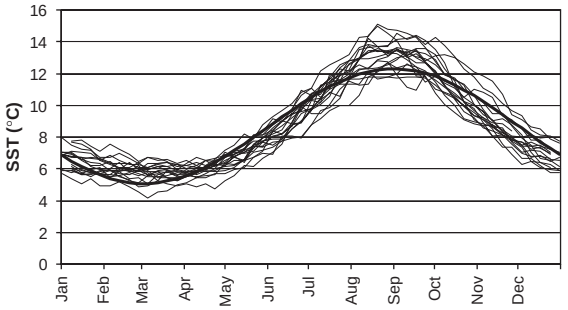

Fig. 4. Weekly average water temperatures for Ocean Station P, shown for each year 1982–1998 (IGOSS, 2000). Dark line shows sine fit to water temperatures used for model runs.

experiments, we consider the arena functional response to be descriptive and not mechanistic (i.e. based on foraging risk): in the absence of explicit recruitment compensation (stock-recruitment curves) or growth compensation for species other than pink salmon, the arena model mimics a null hypothesis of long-term compensatory behavior in modeled fish stocks without specifying the mechanism for each instance of compensation (Aydin, 2004).

Each cohort's numbers and body weight were thus tracked through the year and assumed to leave the gyre on each August 14, followed by the next cohort entering the gyre on August 15 and the process being repeated.

It should be noted that the inputs and model formulation are designed to determine a long-term "steady-state" annual cycle for the interaction of Ocean Station P seasonal dynamics, pink salmon growth, and the other species in the ecosystem. While this baseline cycle might never occur in nature, specific hypotheses can be explored by working from this baseline cycle. Specifically, here we examine how changes in coastal production and carrying capacity, as expressed through varying input numbers or body weights of juvenile salmon, affect maturing salmon growth and other ecosystem components. Further investigation may use this model to examine, for example, the effects seasonal bloom timing, zooplankton production volume, long-term climatic shifts in water temperature, or changes in key predators or prey such as micronektonic squid.

3. Results

3.1. Annual energy flow

The full food web (Ecopath) model of the ESAG is shown in Fig. 5. The parameters of the final model are given in Table A1; sources for parameter values can be found in Aydin et al. (2003). Owing to the inclusion of microzooplankton in the food web model, trophic levels for most species are higher than often reported; for example, copepods are trophic level 2.4; euphausiids are trophic level 3.1 and zooplanktivorous salmon (pink and sockeye) are trophic level 4.2 (Table A1).

On the basis of annual averages of NEMURO-output plankton biomass and production rates, and the consumption rates estimated in the ESAG

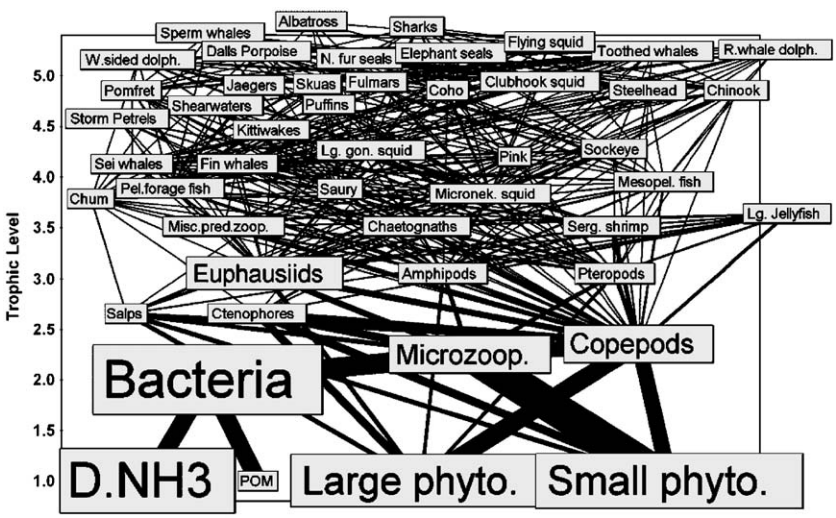

Fig. 5. The eastern Subarctic Pacific Gyre (ESAG) model. Box size is proportional to log(biomass density) of each functional group; although most groups above trophic level 3 show no size differential to allow legibility. The width of each energy (diet) flow line is proportional to the square root of the flow volume.

Ecopath model, small and large phytoplankton have 77% and 67% of their production consumed by other species each year respectively. Microzooplankton are 99% consumed, while copepods are 88% consumed (EE values in Table A1).

The highest trophic level in the NEMURO model, predatory zooplankton, is split into three Ecopath groups; euphausiids, pteropods, and amphipods. In the Ecopath model, these groups have differing biomass levels but identical (NEMURO-output) diets, production and consumption rates: limited diet data are available for these larger zooplankton species. Less of their production is consumed by species of higher trophic levels, with 54% of euphausiid production, 53% of pteropod production, and 64% of amphipod production being consumed annually.

Sergestid shrimp, chaetognaths, and miscellaneous predatory zooplankton are also given the same production and consumption rates from NEMURO, although their diets put them on a higher trophic level in the Ecopath model. Overall these species groups have 19%, 28%, and 19% of their production levels consumed annually in the Ecopath model (Table A1). For the remaining two zooplankton categories, salps and ctenophores, little data exists on these functional groups. With the estimates used in the Ecopath model, very little of these groups' production is consumed, with only 2% of salp production and 5% of ctenophore production passing to higher trophic levels.

The biomass densities of mid-trophic level fish and squid species are shown in Fig. 6 and Table A1. General forage species in the ESAG model were divided into three broad categories; pelagic forage fish, mesopelagic forage fish, and micronektonic squid. By far the largest biomass among these groups was that of mesopelagic fish. Only 16% of mesopelagic fish production was consumed annually; this does not include consumption of mesopelagics by mesopelagics, which is unknown. As no reliable data on pelagic forage fish or micronektonic squid were available, biomass for these two functional groups was calculated by setting the proportion of consumed production (EE) to 90%.

Among the fish and squid of the upper trophic levels, the two species with the highest biomass

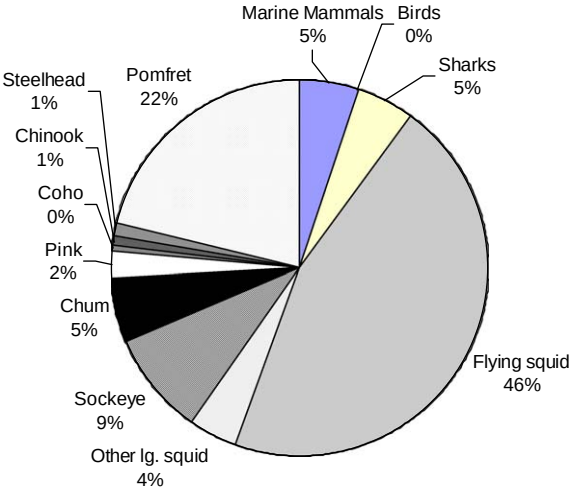

Fig. 6. Biomass composition of functional groups in the ESAG model above trophic level 3.9.

levels were neon flying squid and Pacific pomfret (*Heraclis aesticola*); overall, calculated salmon biomass densities were considerably lower (Fig. 6) than the biomasses of these top species. This is likely a reflection of the location of Ocean Station P, in the southern extreme of the Alaskan Gyre.

Sensitivity analysis in Aydin et al. (2003) of pink salmon to other species demonstrated that under these conditions, salmon would have a relatively minor top-down effect on zooplankton prey when compared to the effect of flying squid; farther to the north (towards the gyre center) salmon influence would be expected to be greater on a per-unit-area basis. Sensitivity analysis of other species on pink salmon indicated that uncertainty in pink salmon itself (biomass and production rates) had a greater effect on the pink salmon predictions than any other trophic component, although bottom-up supply showed a strong effect (see Appendix A).

3.2. Seasonal cycle

Fig. 7A shows daily biomass outputs from the steady-state annual cycle of the NEMURO Ocean Station P model. Ecosim was forced with NEMURO biomass levels for small and large phytoplankton, microzooplankton, and copepods. Fig. 7B shows the annual cycle (daily outputs) of

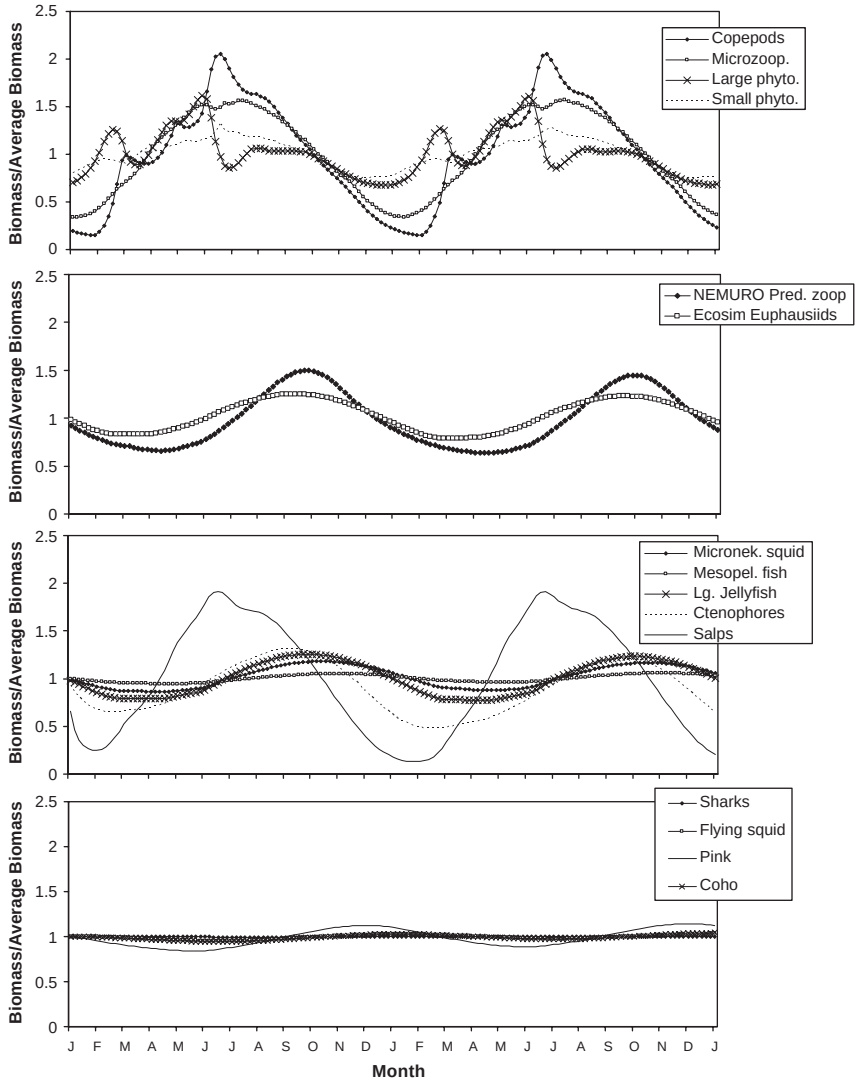

Fig. 7. Ecosim results from two years of a seasonal simulation, with no bioenergetic modeling of pink salmon: (A) plankton inputs from NEMURO model; these were daily model inputs; (B) euphausiids in Ecosim responding to lower trophic level forcing, compared with NEMURO outputs of predatory zooplankton; (C) forage species and gelatinous zooplankton; (D) upper trophic levels including pink salmon.

euphausiids modeled in Ecosim versus predatory zooplankton modeled in NEMURO. Fig. 7C shows the Ecosim-modeled responses of larger zooplankton and forage species, while Fig. 7D shows the response of upper trophic level fish and squid.

As seen in Fig. 7B, the euphausiid seasonal cycle predicted by NEMURO is similar to that predicted by Ecosim when forced by NEMURO. However, Ecosim levels of euphausiids show a lower amplitude of response. In NEMURO, this functional group is the highest trophic level in the model and thus experiences constant mortality, while in Ecosim the effects of upper trophic levels absorbing euphausiid fluctuations can be expected to dampen their annual cycle.

From Fig. 7C, it can be seen that the functional group that shows the greatest response to seasonality are the salps and the ctenophores, due to the combination of being on a low trophic level and experiencing little predation. Overall, in these results, a large proportion of the seasonal variation in system biomass is absorbed by gelatinous zooplankton.

On the higher trophic levels of fish, little variation is seen. Particularly for pink salmon, the base Ecosim model shows little seasonal variability. However, this relies on the default Ecosim assumption that pink salmon resides year-round in the gyres, and thus this version of the model can tell us very little about bottlenecks to salmon production that may occur during a salmon's residence time in the gyres.

3.3. Pink salmon bioenergetics modeling

The annually averaged diet of pink salmon, weighted by consumption rates estimated in Aydin (2000), is shown in Fig. 8. The high preponderance of pteropods and amphipods in this diet is due to the use of December and January data to extrapolate the September–April diet compositions. It was not initially considered whether other species predominate in the fall or the spring.

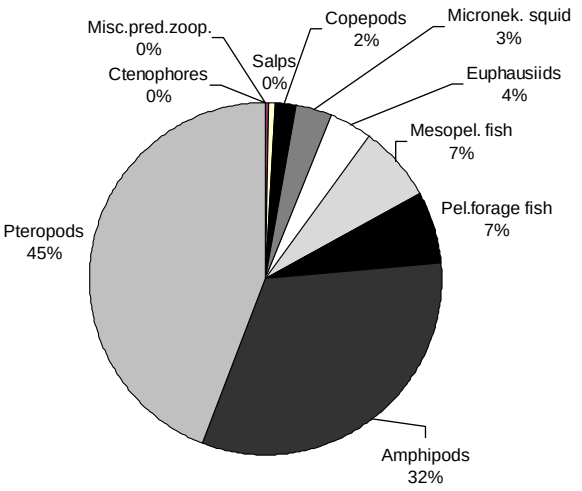

Fig. 8. Annually averaged ocean diet of pink salmon near Ocean Station P, weighted by monthly consumption rates calculated in Aydin (2000). Diets for October–December were assumed to match diets measured in September; Diets for January–April were assumed to match diets measured in December; data existed for all other months.

These averaged diet percentages (DCs) were used in the initial Ecosim/Bioenergetics/NEMURO combined model run, as DCs for the Ecosim foraging equation and a Lotka–Volterra functional response for all pink salmon prey (X_{ij} values $\gg 25$ for pink salmon prey items). Actual diets thus varied by bottom-up control only, as the rate of pink salmon consumption per unit biomass (specific feeding rate) on each prey item was directly proportional to each prey type's biomass in the environment under Lotka–Volterra assumptions.

The resulting modeled seasonal cycle of pink biomass, diets, and body size is shown in Fig. 9. Pink salmon enter the gyres at high numbers and low biomass, resulting in a low biomass of pink salmon overall following their August entry into the gyres. The peak of pink salmon biomass occurs in the winter before mortality reduces biomass faster than somatic growth can replace it (Fig. 9B). The overall yearly production of pink salmon is higher than under the default Ecosim model.

While the initial bioenergetics run reproduced the general growth pattern shown in Ishida et al. (1998), there were a few key differences. Specifically, with the fixed dietary preferences and pure bottom-up seasonal forcing, the salmon grew too rapidly between September and January, yet not rapidly enough between February and July (Fig. 9B). In this base scenario, the final August 14 body weight of salmon, at 939 g, was considerably lower than the reported average August body weight of 1340 g.

It would be possible to fix pink salmon ration and iteratively calculate the foraging rates necessary to force the salmon body weight trajectories to precisely fit observed growth patterns. In fact such iterative fitting was used to produce the initial Ecopath estimate of salmon Q/B rates. However, directly adding this forcing to the dynamic model would remove any mechanistic links between prey supply and salmon foraging behavior, and thus not allow hypotheses testing of the effects of environmental change on salmon growth.

There are also a sufficient number of predator/prey interaction terms to overfit the model and

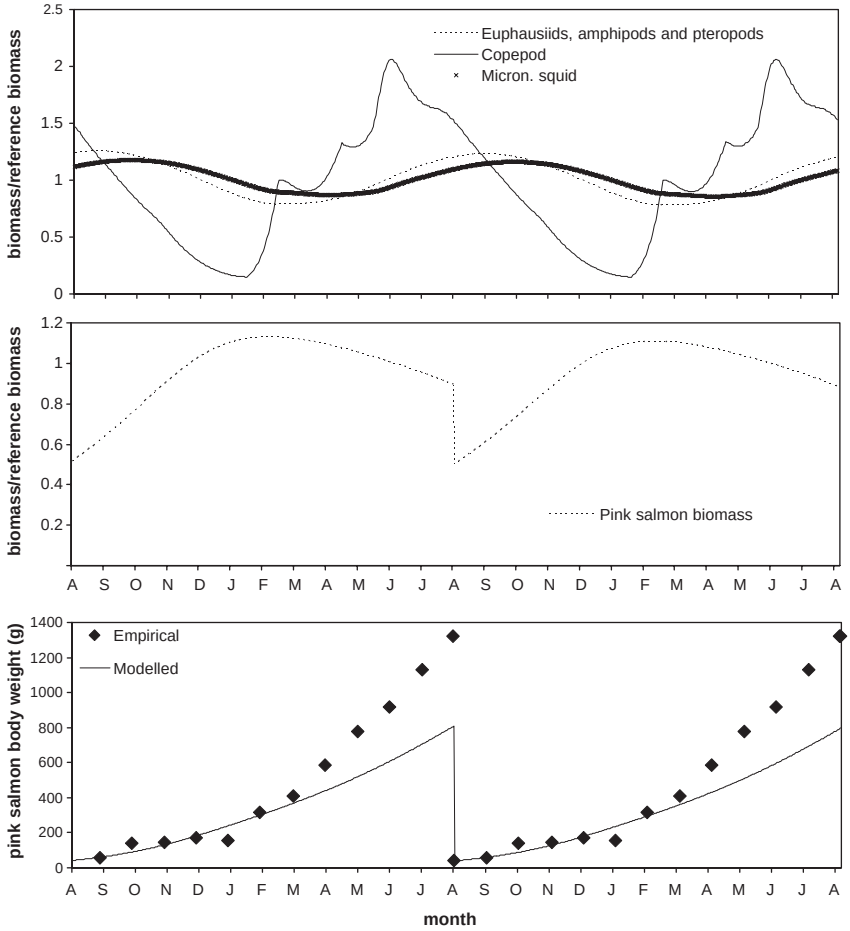

Fig. 9. Results from first run (2 simulated years) of the linked Ecosim/bioenergetics model, assuming annually averaged diets from Fig. 8 to be preferences modified by prey biomass (A) biomass of key prey species; (B) pink salmon biomass; (C) pink salmon body weights compared to empirical measurements.

produce the observed growth, especially if the caloric densities of the different prey items are varied. Rather than attempting to create a precise fit through the variation of all possible parameters, we formulated and tested a set of fairly simple mechanistic hypotheses that might allow the bottom-up controlled foraging rates to respond to the seasonal plankton cycle, and explain both observations of low winter growth and accelerating summer growth of pink salmon based on the input dynamics.

The first set of experiments we performed were to perturb the base Ecopath diet compositions and the total consumption rate (Q/B) of pink salmon. The results of each perturbation was judged using both non-weighted and standard deviation-weighted log sum-of-squares fitting criteria between the measured and output body weights for each month. However, none of these perturbations possessed sufficient explanatory power. In general there was a distinct tradeoff; pink salmon only increased to the measured summer body weights if winter (December–February) body weights of salmon were unrealistically high (Fig. 9C).

Even if copepods were considered to be a major preference in salmon diets, so as to allow pink

salmon to utilize the bloom more effectively, the March–May copepod increase did not provide sufficient food to accelerate somatic growth indicated by the data. In fact, higher preferences for copepods tended to lower growth during the critical early spring, as the salmon replaced the higher-energy amphipods with more numerous but less nutritious copepods in their diets.

Additionally, scenarios of localized density dependence between pink salmon were explored by setting X_{ij} for pink salmon to low values (X_{ij} between 1 and 2 for all pink prey). It was thought that density dependence might have a strong effect during the winter (and produce the lower winter body weights) and the density dependence would be less important in the spring as copepods increased in biomass. However, this also acted against the measured acceleration of pink salmon growth, as the acceleration occurs in early spring when pink salmon overall biomass was highest and thus density-dependent foraging would be greatest (Fig. 9C).

Previous studies of summer pink salmon diets showed that micronektonic squid were a key food source for large pink salmon; in fact, a size-dependent diet switching from plankton to lipid-rich *B. anonychus* was shown by a previous bioenergetics study to greatly accelerate pink and sockeye salmon growth between April and July (Aydin, 2000). The largest salmon therefore would feed on a diet nearly twice as nutritious as smaller zooplankton feeders. The diet data for May and June clearly shows the trend of ontogenetic diet switching—an extremely good body-weight dependent logistic fit was obtained from the 1990s data (Fig. 10). Therefore, this size-dependent ontogenetic diet switch was added into the calculations of diet preference.

However, the midpoint (50% saturation) of the fit logistic curve was at over 1000 g body weight for the pink salmon (Fig. 10); in the initial results, the final body weights of the modeled fish did not reach 900 g until late July or early August, too late for the diet switch to make a difference.

From the 1950–1970 diet dataset (LeBrasseur 1972), some limited sampling of pink salmon occurred in April in the Ocean Station P area (total sample size <10 fish). These samples

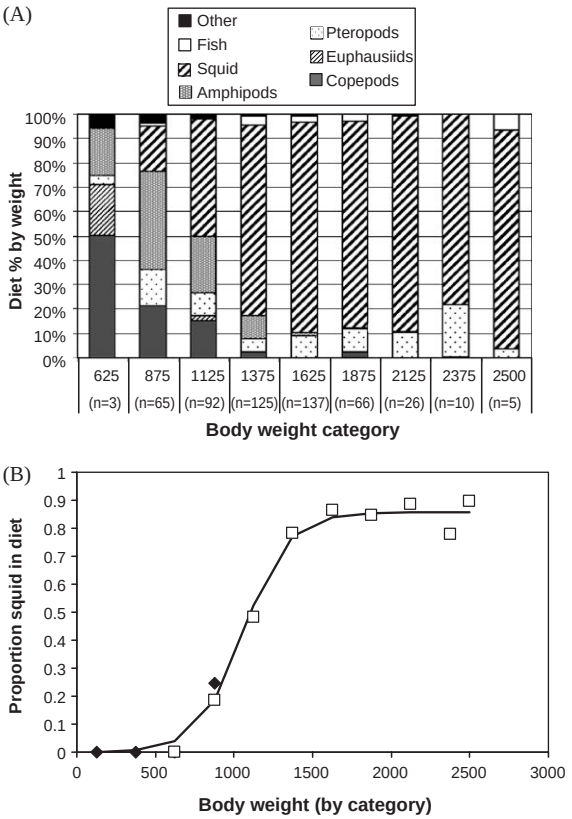

Fig. 10. (A) Pink salmon diets (percent wet weight) near Station P, by body weight in July, from *Oshoro maru* research cruises 1980–2001. (B) Proportion squid in diet as a function of body weight, for May 1998 (solid diamonds) and July 1980–2001 (open squares); Best logistic fit to data (line): $\%\text{squid} = 86\%/(1+e^{-0.0068*(BW-1065\,g)})$.

indicated that fish were a high component of pink salmon diets during this time—if fish are an important diet component for pink salmon in February–April, their higher caloric composition could be sufficient to produce high growth rates. However, to meet the measured body weights later in the season, pink would have to feed on fish through May and June, a time period when 1990s data indicate that they consume primarily zooplankton. But the amount of lower-energy zooplankton they would have to consume, according to the bioenergetics model, would reach their satiation limit.

Therefore, we considered a working hypothesis that some mechanism allows pink salmon to feed on zooplankton in a more energy efficient manner throughout the spring and summer. A change in energy transfer efficiency might arise if the salmon were able to obtain similar quantities of food, but through reduced foraging activity. Recent archival tagging studies of pink salmon indicate that they move throughout the upper 50–70 m of the water column in the summer (Walker et al., 2000), but it is possible that their forage may become concentrated from the shallowing of the mixed-layer depth (MLD).

Mixed-layer depth at Ocean Station P lies between 100 and 150 m depth in the winter, shallowing to the upper 20 m in the summer (Longhurst, 1998). This stratification begins in March and progresses through the springtime. If change in the MLD concentrates plankton on a finer scale than that of the NEMURO results input into the Ecosim model, the increased foraging opportunities for salmon might explain the accelerated growth in springtime even with zooplankton as their primary diet component.

To investigate this possibility, the MLD was input into the predator/prey equations by assuming that the biomass of zooplankton input into Ecosim was spread over the 100 m of the mixed layer (deepest extent). Thereafter, net energetic gains resulting from zooplankton feeding were considered to be inversely proportional to the monthly MLD reported by Longhurst, 1998, as concentration of zooplankton would reduce the energy requirements of foraging salmon for a given ration. Energetic gains from fish and squid were not set by MLD: as these species are mesopelagic, the MLD-induced concentration of prey would be limited. In this run of the model, the ontogenetic diet switch to micronektonic squid was also included.

The results of this run are shown in Fig. 11. The zooplankton concentration with MLD, which increases salmon foraging costs in the winter and decreases foraging costs in the summer, in

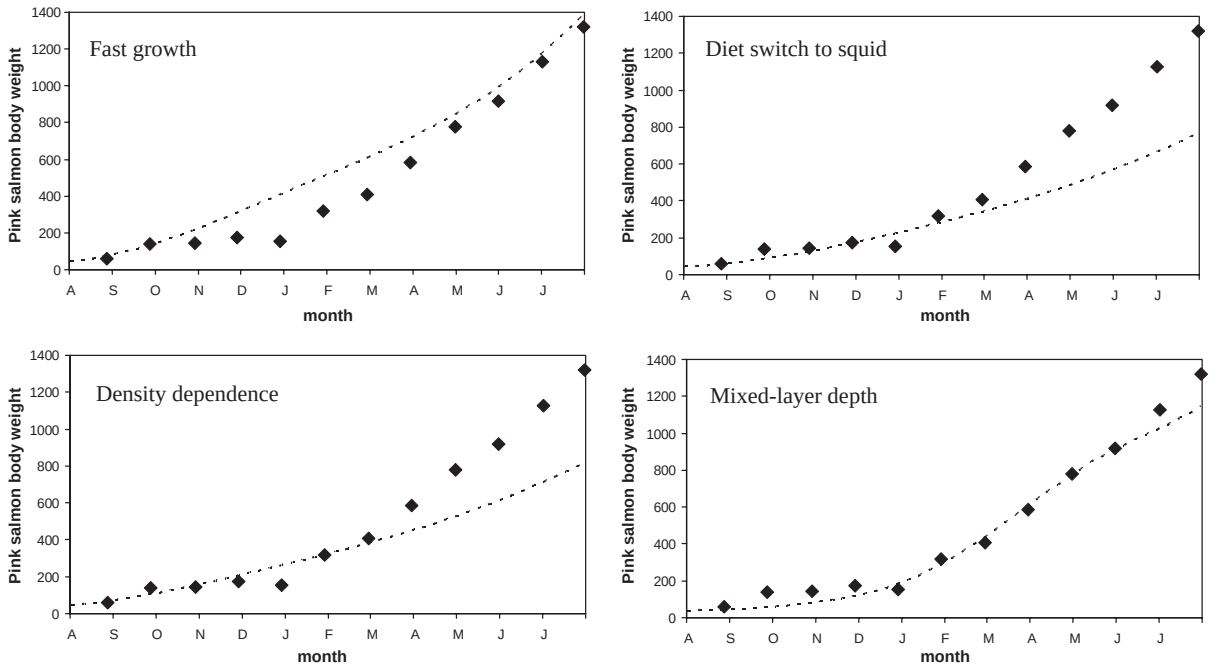

Fig. 11. Comparison of predicted pink salmon body weights to actual body weights for 4 model scenarios: fast growth (best fit to summer body weights by increasing base pink salmon Q/B); density-dependence (pink-salmon prey X values set to 2.0); switch to squid feeding based on body weight; foraging efficiency inversely proportional to mixed-layer depth, including switch to squid feeding.

combination with the ontogenetic diet shift in squid, best reproduces the observed pattern of winter and summer growth in pink salmon at Ocean Station P.

With this final model including MLD-linked energetic changes and ontogenetic diet shifts, we explored the influence of coastal processes by varying (1) the initial body weight of entering salmon by ±10% and (2) the entrance date of salmon into the model by ±30 days. In the final base model, the simulated body weight of salmon exiting the gyre was 1305 g. A 10% increase/decrease in entering salmon body weight led to a 4% increase/decrease in final body weights (1356 and 1250 g, respectively). Fish entering the gyre 30 days earlier/later showed a 0.8% increase/decrease in final body weights (1315 and 1296 g, respectively). The effects were more or less additive, as a fish entering both 30 days early and 10% larger showed a final body weight increase of 5% (1367 g). Adding explicit density dependent effects to growth via the functional responses did not greatly affect these results.

4. Discussion

Based on the model fitting performed above, we suggest a preliminary hypothesis for food web factors controlling adult ocean growth of pink salmon. Seasonal changes in pink salmon/prey interactions, due to changes in predator/prey overlap in the water column with the seasonal cycle of the mixed-layer depth, may explain the previously measured pattern of slow winter growth and accelerated summer growth in the Alaskan Gyre, which is not explained by biomass-driven bottom-up forcing alone. In late summer, an ontogenetic diet switch from zooplankton to micronektonic squid is required to maintain high growth rates (Fig. 11).

The annual balance of consumption and growth rates suggest that, while salmon are a relatively small component of the waters around Ocean Station P, there is a high plankton utilization by other species, especially gelatinous zooplankton. When the seasonal cycle was modeled, a large proportion of the production variation was absorbed by ctenophores and salps (Fig. 7). This situation may differ substantially in the northern portion of the gyre where salmon are more numerous.

Overall, pink salmon in the gyre Ecosim model were more sensitive to bottom-up effects than top-down or competitive effects (Figs. A1 and A2). As the bottom-up forcing in this combined model is entirely determined by NEMURO, a more complete set of variations in NEMURO inputs would be the logical next step for further evaluating these hypotheses.

A sensitivity analysis on the bioenergetics inputs' relationship to final pink salmon body weights shows four input variables which had an effect on the results: entry day of salmon into the gyre, entering salmon body weight, average water temperature (throughout year), amplitude of temperature variations (colder winters and warmer summers), and prey caloric density (Table 4). The sensitivities are reported for the final body weight only, and not to the relative fits for the hypotheses for growth patterns throughout the year.

Final body weight was most sensitive to the caloric content of the prey, indicating that diet

Table 4
Percent change in final pink salmon body weight with ±10% change in input bioenergetics parameters

Parameter	Base	+10%	−10%
Salmon entry day	228 (Julian day)	−0.8%	+1.1%
Starting body weight	39.5 g	+3.8%	−4.1%
Average water temperature	8.68 °C	−2.8%	+1.1%
Seasonal temperature amplitude	3.16 °C	−1.2%	+1.1%
Prey cal/gram wet weight	Varies by diet item	+24.3%	−22.1%

Baseline is the final pink salmon body weight of 1305 g from the final model, which includes both a seasonal mixed layer depth changes and prey switching.

switching and competition with other Pacific salmon species over high-energy food may be substantial, even if other salmon do not have a large effect on pink biomass when modeled using the biomass-based Ecosim model alone (Fig. A2).

The effect of entry weight on final body size is noticeable, and larger than the direct effect of water temperature. The effect is reduced over time, in that 10% variation in input values leads to a 4% variation in results (Table 4). This contrasts with Aydin (2000), in which only April–July growth was modeled. In that case, given a fixed MLD, the April body weight of pink salmon had a strong (amplifying) effect on July and August body weights due to the ontogenetic diet switch: an April difference of 10% led to a 50–100% difference in final body weights. This contrast in results may be due to separating the winter/spring effects from the late summer accelerated growth period. In either case, if coastal carrying capacity affects entry body weight, the initial density-dependent effects on salmon production may remain throughout the year.

As previously noted by Aydin et al. (2000), correlations between water temperature and salmon production may be proxies for predator/prey processes such as the biogeographic overlap of prey or variation in timing of mixed layer depth changes. This model may be used to further explore these possibilities, especially if other salmon species are included in the explicit bioenergetics modeling. Moreover, MLD and temperature would have an effect on timing and development of plankton (Mackas et al., 1998), so the next set of explorations should connect physical factors through both NEMURO and the combined model presented here.

It should be noted that a model, especially a complex model, should be seen as a tool for hypothesis falsification and exploration rather than a confirmatory tool. For example, the results here indicate that diet switching alone is less likely to result in the measured pattern of salmon growth than diet switching coupled with MLD changes; however, this does not preclude other mechanisms such as differential size-based mortality in salmon, or changes in zooplankton bloom timing (e.g., Mackas et al., 1998). However, the flexibility of the linked models described in this paper should allow additional hypotheses to be tested as they are developed.

This spatial aspect, in particular, should be the next step in extending these models. In particular, salmon may migrate depending on growth conditions, body weight, or maturity schedule, through varying oceanographic regions that further partition the subarctic gyres. Including dynamics in an explicitly spatial manner would extend the capabilities of this model with respect to salmon.

5. Conclusions

The results presented here stress the need for direct comparisons of multiple models, either through explicit linkages, input drivers, or side-by-side examination. The difference between euphausiid dynamics, in NEMURO where they are a top predator and in Ecosim where they are near the bottom, illustrates the need for two-way feedback; Ecosim is an inappropriate model for explicitly simulating the detailed nutrient dynamics captured in NPZ models, but it can provide the feedback of varying top-down control for the lower trophic levels.

The ''whole food web'' dynamic modeling approach differs from many others, in that it begins with an overarching picture of an ecosystem. The nature of such a picture is that it is averaged on many scales, seasonal and spatial, and as such may be considered overly unrealistic. However, as opposed to ''bottom-up'' process models such as NPZ, this method allows researchers to assess the importance of detailed interactions in progressive stages.

For example, for Pacific salmon in the subarctic Pacific, micronektonic squid are an important late-season food source, and our limited knowledge of this functional group initially precludes detailed modeling. Starting with the big picture presented in the food web, seasonal and spatial detail can be added in a stepwise manner as done for pink salmon in this study until the necessary interactions are covered. It is expected that this process of building model linkages across scales will be a

critical activity in examining interactions between climate, seasons, and marine ecosystems.

Appendix A. Model sensitivity

Ecosim is a complex model, and like all complex models the sensitivity of the model to input assumptions should be carefully assessed. It is beyond the scope of this paper to assess sensitivities of the Ecosim methodology in general: we confine ourselves to the sensitivity of the model to predictions of pink salmon biomass, given uncertainty in input data. Sensitivity of the results of the combined NEMURO–ECOSIM bioenergetics models to bioenergetics assumptions are described in the main text.

Uncertainty in results was measured through a multistep process. The first was to assess, in a workshop setting, the relative quality of input data (variation range or the "data pedigree") based on knowledge of sampling methodology and coverage, with input from a range of data providers. A report of this process may be found in Aydin et al. (2003). Once the data quality was assessed, model constraints were added using the Ecotrophic Efficiency (EE) parameter through the Ecopath balancing process (Polovina, 1985; Christensen et al., 2000).

An EE > 1.0 indicates that a functional group's annual accounted losses are greater than its accounted gains. The preferred method for using the Ecopath model is to input all parameters from independent data sources, except for EE in each functional group. Ecopath will calculate an implied EE for each group by solving the resulting set of linear equations, utilizing the generalized inverse method (Mackay, 1981) to guarantee a solution. The estimation of EE is thus the primary tool for data calibration in Ecopath: independent estimates of consumption and production of different species often lead to initial conclusions that species are being preyed upon more than they are produced (EE > 1.0), which is impossible under the mass-balance assumption (Christensen et al., 2000); actual measured biomass change should be included in the accounting through the biomass accumulation (BA) term.

By using an EE > 1.0 as a diagnostic tool for error, it is possible to assess the relative quality of each piece of input data to adjust inputs to a self-consistent whole. This process is known as "balancing" the model: it does not imply that the true ecosystem is in equilibrium but rather

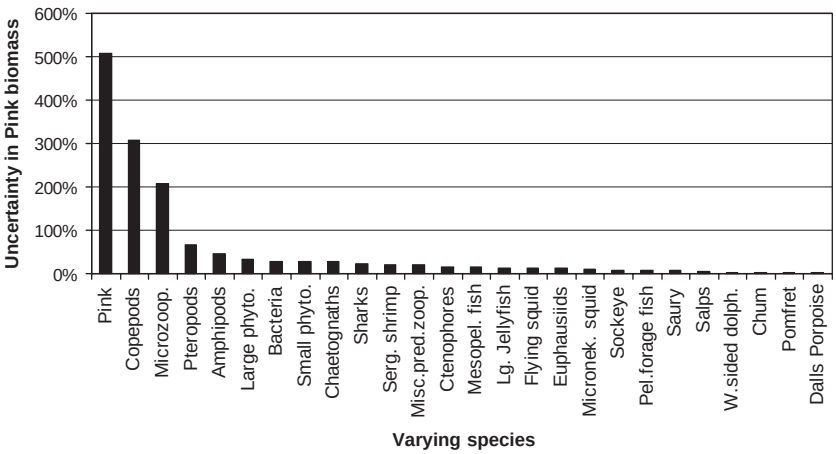

Fig. A1. Variation in pink salmon equilibrium biomass caused by variation in each species' input values, sorted by magnitude of pink salmon variation. For each bar, 10,000 ecosystems were generated using a Monte Carlo routine, with the "varying species" parameters varying throughout its range of variation as determined by its data pedigree. The bars show the width of the 95% confidence interval of pink salmon biomass, as a percentage of initial Ecopath biomass. Only species causing more than 1% variation in pink salmon are shown.

quantifies the uncertainty contained in the estimates of supply and demand present in the system. In cases where the initial eastern Subarctic Gyre model was out of balance, data were adjusted within the range of their pedigree. It is worth noting that the resulting model (Table A1) showed few changes from the initial inputs, and the differences were mainly due to "range overlap" errors in which data were used from different subregions of the broad subarctic gyres.

By treating the data pedigrees as prior distributions, Monte Carlo or Bayesian Synthesis techniques may be used to assess uncertainty. Here, two results are presented with respect to pink salmon.

In Fig. A1, ecosystems were generated randomly, and each constrained to exhibit the basic thermodynamic criteria of long-term persistence of all species as some (varying) positive equilibrium level (the Ecosense routines; Aydin et al., 2003). Each species was permitted to vary in turn according to the assessed variance in its input variables (biomass, P/B, Q/B, and diet), and 10,000 models for each species were generated and the equilibrium (stable Ecopath) biomasses were determined for each model.

Fig. A1 shows the result with respect to pink salmon only, sorted by descending level of variation. The metric plotted is the width of the 95% confidence interval for the 10,000 models, as a percentage of the initial Ecopath equilibrium biomass. Uncertainty in pink salmon input variables caused the greatest variation in pink salmon equilibrium biomass. Copepods and microzooplankton also caused a large variability in pink salmon.

In Fig. A2, all species' input values were simultaneously varied according to their pedigree, and 10,000 ecosystems were generated. In each of these 10,000 ecosystems, the effect on pink salmon biomass of perturbing each species upwards was measured, and the difference median difference across ecosystems is shown. Again, pink salmon have the largest effect (on themselves) and bottom-up effects show the next level of impact. Top-down and competitive (negative) effects were relatively minor. One interesting note is that copepods as a major source of variation in Fig. A1 but not A2: while variation in copepods causes large variation in pink salmon, the median direction of pink salmon biomass, under conditions of a copepod increase, across ecosystems, varies with a median near zero: in many generated ecosystems, increases in copepods primarily benefits species other than pink salmon.

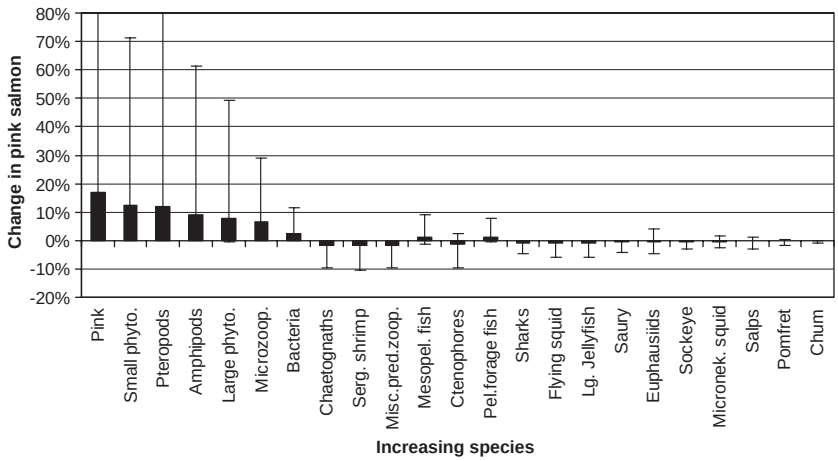

Fig. A2. Median (bars) and 95% confidence interval of the percent change in equilibrium biomass of pink salmon as a result of increasing each species in turn by 10% while all species' inputs vary throughout their pedigree range. 95% confidence intervals were calculated from 10,000 Monte Carlo runs performed for each species' increase. Species are shown by the absolute value of their median effect on pink salmon: species with median effects less than 0.1% are not shown.

Table A1
Parameters and estimated values for the ESAG ECOPATH model. Shaded values were estimated by the model. Shown are: trophic level (TL), biomass (B, t/km^2), production/biomass (P/B, 1/year), consumption/biomass (Q/B, 1/year), ecotrophic efficiency (EE, propotion)

Group	TL	B	P/B	Q/B	EE
Sperm whales	5.4	0.000929	0.0596	6.61	0
Toothed whales	5.2	0.000028	0.0252	11.16	0
Fin whales	4.1	0.027883	0.02	4.56	0.12912
Sei whales	4.1	0.005902	0.02	6.15	0.1358
N. fur seals	5.2	0.000246	0.235	39.03	0.01083
Elephant seals	5.2	0.00043	0.368	11.08	0.00692
Dalls porpoise	5.2	0.00598636	0.1	27.47	0.02546
W. sided dolph.	5.2	0.00396248	0.14	25.83	0.01819
R. whale dolph.	5.3	0.00389728	0.16	24.14	0.01592
Albatross	5.9	0.00004	0.05	81.59	0.05043
Shearwaters	4.7	0.0004	0.1	100.13	0.02547
Storm Petrels	4.6	0.000056	0.1	152.08	0.02546
Kittiwakes	4.6	0.000052	0.1	123	0.02549
Fulmars	4.9	0.000074	0.1	100.26	0.02557
Puffins	4.7	0.000058	0.1	104.33	0.02535
Skuas	4.8	0.000054	0.075	96.6	0.0338
Jaegers	4.8	0.000038	0.075	96.6	0.03388
Sharks	5.4	0.05	0.2	10.95	0
Lg. gon. Squid	4.2	0.03	2.555	7.3	0.19453
Clubhook squid	4.9	0.012	2.555	7.3	0.19453
Flying squid	5.3	0.45	2.555	6.205	0.91095
Sockeye	4.3	0.08965573	1.27	10.13	0.32249
Chum	3.7	0.05413587	1.93	14.51	0.21221
Pink	4.2	0.02326662	3.37	18.49	0.12153
Coho	4.9	0.00445349	2.47	16.55	0.16581
Chinook	4.9	0.00930315	0.8	5.33333	0.51195
Steelhead	4.9	0.0093	0.8	5.33333	0.51212
Pomfret	4.8	0.21	0.75	3.75000	0.54697
Saury	3.8	0.45	1.6	7.9	0.5545
Pel.forage fish	3.9	0.92156	1.5	5	0.9
Micronek. Squid	3.9	0.87135	3	15	0.9
Mesopel. Fish	3.9	4.5	0.9	3	0.16002
Lg. Jellyfish	3.6	4	3	10	0
Ctenophores	2.7	9.1	4	110	0.05269
Salps	2.7	8	9	30	0.02371
Chaetognaths	3.5	6.6	2.555	12.045	0.27638
Serg. Shrimp	3.5	5	2.555	12.045	0.18813
Misc.pred.zoop.	3.5	5.0688	2.555	12.045	0.18871
Amphipods	3.1	10.1376	2.555	12.045	0.64429
Pteropods	3.1	10.1376	2.555	12.045	0.53491
Euphausiids	3.1	25.344	2.555	12.045	0.53934
Copepods	2.4	34.848	23.725	112.42	0.88106
Microzoop.	2.3	35	48.91	233.235	0.99619
Bacteria	2	122.90310	18.45	25	0.9
Large phyto.	1	69.7	42.34		0.67337
Small phyto.	1	76	129.575		0.77256
DNH3	1				0.42757
POM	1				0.42757

References

Atkinson, K.E., 1989. An Introduction to Numerical Analysis, second ed. Wiley, New York 693pp.

Aydin, K.Y., 2000. Trophic feedback and carrying capacity of Pacific salmon (*Oncorhynchus* spp.) on the high seas of the Gulf of Alaska. Ph.D. Dissertation, University of Washington, Seattle. 392pp.

Aydin, K.Y., 2004. Age structure or functional response? Reconciling the energetics of surplus production between single-species models and Ecosim. African Journal of Marine Science 26, 289–301.

Aydin, K.Y., Myers, K.W., Walker, R.V., 2000. Variation in summer distribution of the prey of Pacific salmon (*Oncorhynchus* spp.) in the offshore Gulf of Alaska in relation to oceanographic conditions, 1994–98. North Pacific Anadromous Fish Commission Bulletin 2, 43–54.

Aydin, K.Y., McFarlane, G.A., King, J.R., Megrey, B.A., 2003. The BASS/MODEL Report on trophic models of the subarctic Pacific basin ecosystems. North Pacific Marine Science Organization (PICES) Report #25, 93pp.

Beamish, R.J., 1993. Climate and exceptional fish production off the west coast of North America. Canadian Journal of Fisheries and Aquatic Sciences 50, 2270–2291.

Beamish, J.R., Mahnken, C., 2001. A critical size and period hypothesis to explain natural regulation of salmon abundance and the linkage to climate and climate change. Progress in Oceanography 49, 423–437.

Beamish, R.J., Noakes, D.J., McFarlane, G.A., Klyashtorin, L., Ivanov, V.V., Kurashov, V., 1999. The regime concept and natural trends in the production of Pacific salmon. Canadian Journal of Fisheries and Aquatic Sciences 56, 516–526.

Beauchamp, D.A., Stewart, D.J., Thomas, G.L., 1989. Corroboration of a bioenergetics model for sockeye salmon. Transactions of the American Fisheries Society 118, 597–607.

Bigler, B.S., Welch, D.W., Helle, J.H., 1996. A rewiew of size trends among North Pacific salmon (*Oncorhynchus* spp.). Canadian Journal of Fisheries and Aquatic Sciences 53, 455–465.

Bradford, M.J., 1995. Comparative review of Pacific salmon survival rates. Canadian Journal of Fisheries and Aquatic Sciences 52, 1327–1338.

Brodeur, R.D., Ware, D.M., 1995. Interdecadal variability in distribution and catch rates of epipelagic nekton in the Northeast Pacific Ocean. In: Beamish, R.J. (Ed.), Climate Change and Northern Fish Populations. National Research Council of Canada, Ottawa, pp. 329–356.

Brodeur, R., McKinnell, S., Nagasawa, K., Pearcy, W., Radchenko, V., Takagi, S., 1999. Epipelagic nekton of the North Pacific Subarctic and Transition Zones. Progress in Oceanography 43, 365–398.

Christensen, V., Pauly, D., 1992. ECOPATH II—a software for balancing steady-state ecosystem models and calculating network characteristics. Ecological Modelling 61, 169–185.

Christensen, V., Walters, C.J., Pauly, D., 2000. ECOPATH with ECOSIM: a Users Guide, October 2000 Edition. Fisheries Centre, University of British Columbia, Vancouver, Canada and ICLARM, Penang, Malaysia, 130pp.

Cox, S.P., Essington, T.E., Kitchell, J.F., Martell, S.J.D., Walters, C.J., Boggs, C., Kaplan, I., 2002. Reconstructing ecosystem dynamics in the central Pacific Ocean, 1952–1998. II. A preliminary assessment of the trophic impacts of fishing and effects on tuna dynamics. Canadian Journal of Fisheries and Aquatic Sciences 59, 1736–1747.

Davis, N.D., 2003. Feeding Ecology of Pacific salmon (*Oncorhynchus* spp.) in the Central North Pacific Ocean and Central Bering Sea, 1991–2000. Ph.D. Dissertation, Hokkaido University, Hakodate, Japan, 190pp.

Favorite, F., Laevastu, T., 1979. A study of the Ocean Migrations of Sockeye Salmon and Estimation of the Carrying-Capacity of the North Pacific Ocean using a Dynamical Salmon Ecosystem Model (NOPASA). NWAFC Processed Report 79–16. Northwest and Alaska Fisheries Center, NMFS, Seattle, WA (47pp).

Francis, R.C., Hare, S.R., Hollowed, A.B., Wooster, W.S., 1998. Effects of interdecadal climate variability on the oceanic ecosystems of the NE Pacific. Fisheries Oceanography 7, 1–21.

Fujii, M., Nojiri, Y., Yamanaka, Y., Kishi, M.J., 2002. A one-dimensional ecosystem model applied to time series Station KNOT. Deep-Sea Research II 49, 5411–5461.

Heard, W.R., 1991. Life history of pink salmon (*Oncorhynchus gorbuscha*). In: Groot, C., Margolis, L. (Eds.), Pacific Salmon Life Histories. University of British Columbia Press, Vancouver, BC., pp. 119–230 (564pp).

Hewett, S.W., Johnson, T.B., 1992. A generalized bioenergetics model of fish growth for microcomputers. University of Wisconsin Sea Grant Institute, Madison, Wisconsin. UW Sea Grant Tech. Rep. WIS-SG-92-250, 79pp.

Hollowed, A.B., Hare, S.R., Wooster, W.S., 1998. Pacific—basin climate variability and patterns of northeast Pacific marine fish production. In: Holloway, G., Muller, P., Henderson, D. (Eds.), Proceedings of the 10th 'Aha Huliko'a Hawaiian winter workshop on biotic impacts of extratropical climate variability in the Pacific. January 26–29, 1998. SOEST Special Publication, pp. 89–104.

IGOSS (Integrated Global Ocean Services System Products Bulletin), 2000. Joint WMO/IOC Technical Commission for Oceanography and Marine Meteorology.

Ishida, Y., Ito, S., Kaeriyama, M., McKinnell, S., Nagasawa, K., 1993. Recent changes in age and size of chum salmon (*Oncorhynchus keta*) in the North Pacific Ocean and possible causes. Canadian Journal of Fisheries and Aquatic Sciences 50, 290–295.

Ishida, Y., Ito, S., Ueno, Y., Sakai, J., 1998. Seasonal growth patterns of Pacific salmon (*Oncorhynchus* spp.) in offshore waters of the North Pacific Ocean. North Pacific Anadromous Fish Commission Bulletin 1, 66–80.

Kaeriyama, M., Nakamura, M., Edpalina, R., Bower, R., Yamaguchi, H., Walker, R.V., Myers, K.W., 2004. Change in feeding ecology and trophic dynamics of Pacific salmon

(*Oncorhyncus* spp.) in the central Gulf of Alaska in relation to climate events. Fisheries Oceanography 13, 197–207.

LeBrasseur, R.J., 1966. Stomach contents of salmon and steelhead trout in the northeastern Pacific Ocean. Journal of the Fisheries Research Board of Canada 23, 85–100.

LeBrasseur, R.J., 1972. Utilization of herbivore zooplankton by maturing salmon. In: Takenouti, A.Y. (Ed.), Biological Oceanography of the Northern Pacific Ocean. Idemitsu Shoten, Tokyo, pp. 581–588.

Longhurst, A., 1998. Ecological Geography of the Sea. Academic Press, San Diego, CA (398pp).

Mackas, D.L., Goldblatt, R., Lewis, A.G., 1998. Interdecadal variation in developmental timing of Neocalanus plumchrus populations at Ocean Station P in the subarctic North Pacific. Canadian Journal of Fisheries and Aquatic Sciences 55, 1878–1893.

Mackay, A., 1981. The generalized inverse. Practical Computing, 108–110.

Mantua, N.J., Hare, S.R., Zhang, Y., Wallace, J.M., Francis, R.C., 1997. A Pacific interdecadal climate oscillation with impacts on salmon production. Bulletin of the American Meteorological Society 78, 1069–1080.

Myers, K.W., 1993. Japan, USA, and Canada cooperatuve survey on overwintering salmonids in the North Pacific Ocean: *Kaiyo Maru*, Cruise Report, 25 November–24 December 1992. Fisheries Research Institute, University of Washington, FRI-UW Doc. No. 9301, 16pp.

Myers, K.W., 1996. Survey on overwintering salmonids in the North Pacific Ocean: *Kaiyo Maru*, Cruise Report, 5 January–29 January 1996. Fisheries Research Institute, University of Washington, FRI-UW Doc. No. 9607, 54pp.

Ocean Carrying Capacity Program, 1998. Research plan for the United States Research Vessel Great Pacific in the eastern North Pacific Ocean April–May 1998. (NPAFC Doc. 304) Available from Auke Bay Laboratory, Alaska Fisheries Science Center, NMFS, NOAA, 11305 Glacier Highway, Juneau, AK 99801–8626.

Pauly, D., Christensen, V. (Eds.), 1996. Mass-balance models of north-eastern Pacific ecosystems. Fisheries Centre, University of British Columbia, Research Reports 4, 131pp.

Pearcy, W.G., Brodeur, R.D., Shenker, J.M., Smoker, W.W., Endo, Y., 1988. Food habits of Pacific salmon and steelhead trout, mid-water trawl catches and oceanographic conditions in the Gulf of Alaska, 1980–85. Bulletin of the Ocean Research Institute 26, 29–78.

Pearcy, W.G., Aydin, K.Y., Brodeur, R.D., 1999. What is the carrying capacity of the North Pacific Ocean for salmonids? PICES press vol. 7(2), pp. 17–23.

Polovina, J.J., 1985. An approach to estimating an ecosystem box model. Fisheries Bulletin US 83, 457–460.

Ricker, W.E., 1995. Trends in the average size of Pacific salmon in Canadian catches. In: Beamish, R.J. (Ed.), Climate Change and Northern Fish Populations. Canadian Special Publication of Fisheries and Aquatic Sciences, vol. 121. pp. 593–602, 739pp.

Rogers, D., 2001. Estimates of Annual Salmon Runs from the North Pacific, 1951–2001. Fisheries Research Institute, University of Washington, Document #0115, 11pp.

Sanger, G.A., 1972. Fishery potentials and estimated biological productivity of the subarctic Pacific region. In: Takenouti, A.Y. (Ed.), Biological Oceanography of the Northern North Pacific Ocean. Idemitsu Shoten, Tokyo, pp. 561–574 (626pp).

Shannon, L.J., Cury, P.M., Jarre, A., 2000. Modelling effects of fishing in the Southern Benguela ecosystem. ICES Journal of Marine Science 57, 720–722.

Walker, R.V., Myers, K.W., Davis, N.D., Aydin, K.Y., Friedland, K.D., Carlson, H.R., Boehlert, G.W., Urawa, S., Ueno, Y., Anma, G., 2000. Ambient temperatures and diurnal behavior as indicated by data storage tags on salmonids in the North Pacific. Fisheries Oceangraphy 9, 171–186.

Walters, C., Christensen, V., Pauly, D., 1997. Structuring dynamic models of exploited ecosystems from trophic mass-balance assessments. Reviews in Fish Biology and Fisheries 7, 139–172.

Welch, D.W., Ishida, Y., Nagasawa, K., 1998. Thermal limits and ocean migrations of sockeye salmon (*Oncorhynchus nerka*): long-term consequences of global warming. Canadian Journal of Fisheries and Aquatic Sciences 55, 937–948.

Wong, C.S., Whitney, F.A., Iseki, K., Page, J.S., Zeng, J., 1995. Analysis of trends in primary production and chlorophyll-a over two decades at Ocean Station P (50°N, 145°W) in the subarctic Northeast Pacific Ocean. In: Beamish, R.J. (Ed.), Climate Change and Northern Fish Populations, Canadian Special Publication of Fisheries and Aquatic Sciences, vol. 121. pp. 107–117.

Yamanaka, Y., Yoshie, N., Fujii, M., Aita, M.N., Kishi, M.J., 2003. An ecosystem model coupled with nitrogen–silicon–carbon cycle applied to Station A-7 in the Northwestern Pacific. Journal of Oceanography 60, 227–241.